Silica-coated Metallic Nanoparticle-based Hierarchical Super-hydrophobic Surfaces Fabricated by Spin-Coating and Inverse Nanotransfer Printing

Shengjie Zhai and Hui Zhao[a]

Department of Mechanical Engineering University of Nevada, Las Vegas, NV, United States, 89154

By combining spin coating and inverse nanotransfer printing, silica-coated gold nanoparticles are patterned onto PDMS super-hydrophobic surfaces to form the hierarchical structure. A layer of nanoparticles is spin-coated on a flat silicon substrate serving as the stamp, which is then transferred to the raised regions of PDMS surfaces. Our inverse nanostransfer printing is in contrast to the standard nanotransfer printing which transfers metal from the raised regions of a stamp to a flat PDMS surface. The fabricated hierarchical surface exhibits a higher contact angle and delays the Cassie-Wenzel transition during evaporation of a sessile droplet, indicating an improvement of super-hydrophobicity. Finally, we demonstrate that the fabricated nanoparticle-based super-hydrophobic surfaces can enhance the Raman intensity and significantly decrease the surface-enhanced Raman scattering (SERS) detection limit.

[a] All correspondence should be directed to this author (hui.zhao@unlv.edu)

Super-hydrophobic surfaces covered with micro or nano structures (such as posts, grooves, or holes) can effectively trap bubbles.[1,2] If liquid surface contact is restricted to the top of the roughness, known as the Cassie state, the liquid will be in contact with the solid only over a fraction of the surface, resulting in drag reduction, facilitation of heat transfer, self-cleaning, anti-corrosion, anti-sticking, and anti-contamination. They have opened many exciting opportunities in marine technology, automotive, biosensing, and lab-on-a-chip technologies.[3–6]

Experiments suggested that super-hydrophobic surfaces with metallic nanostructures can break the diffusion limit and detect molecules at femto- or attomolar solutions,[5,7] if droplets over super-hydrophobic surfaces maintain quasi-spheres during evaporation and do not wet the surface, because this way can effectively localize molecules and decrease the detection limit of plasmonic nanosensors. Hence the integration of metallic nanostructures and super-hydrophobic surfaces can pave the road towards developing high-sensitive, label-free, and miniaturized biosensors with potential applications ranging from early disease diagnosis to fast sequence of genomes.[8] Currently, metallic nanoparticles were decorated over super-hydrophobic surfaces by electron-beam lithography which is expensive and not suitable for the large-scale fabrication, limiting its applications.

In addition, for droplets to remain quasi-spherical, the surface needs to stay in the Cassie state. However, it is recognized that the transition from the Cassie state to the Wenzel state (a fully wetting state) during evaporation can be triggered under certain conditions including high pressure.[9] Once the surface is fully wetted, the advantages of the super-hydrophobicity like self-cleaning will lose. In other words, a strategy to delay this transition is highly desirable to fully exploit super-hydrophobic surfaces. Recent studies revealed that super-hydrophobic surfaces

with hierarchical structures consisting of both microstructure and nanostructure can increase the contact angle and improve the stability and robustness of such surfaces.[10–13] Interestingly, patterned nanoparticles can play a dual role. On one hand, they serve as the plasmonic sensors; on the other hand, they promote the super-hydrophobicity and improve the sensitivity of the detection. Hence, it is important to develop a cost-effective and scale-up method to pattern metallic nanostructures onto super-hydrophobic surfaces and assure that such surfaces can maintain the Cassie state as long as possible during evaporation.

In this letter, we describe a simple fabrication technique to transfer nanoparticles onto a super-hydrophobic surface. Our method consists of two key steps. First we apply a spin-coating method developed by Jiang et al.,[14–17] where they generate a monolayer or multilayer of colloidal latex particles by spin-coating. Here we spin-coat gold nanoparticles onto the silicon wafer. Next, we modify the nanotransfer printing technique[18–22] which transfers metal from the raised regions of the rigid stamp onto a flat PDMS surface. Instead, we transfer gold nanoparticles from the flat rigid stamp onto the raised regions of a PDMS structured surface by bringing them into intimate physical contact. We coin our method as inverse nanotransfer printing.

Our method is simple, low-cost and ready to scale up. In this letter, we pattern nanoparticles onto super-hydrophobic surfaces and demonstrate that the hierarchical surface with nanoparticles enhances super-hydrophobicity by both effectively increasing the contact angle and delaying the Cassie-Wenzel transition.

First, we spin-coated a layer of gold nanoparticles onto the silicon wafer. 70 nm gold nanoparticles coated with 10 nm hydrophobic silica shell were purchased from Ted Pella inc. The silica shell is intended to prevent the aggregation of colloidal gold nanoparticles. In order to

spin-coat a uniform layer of nanoparticles, the silicon substrate was treated by 3-acryloxypropyl trichlorosilane (APTCS) .[23]

Figure 1a presents the procedures for uniformly patterning a layer of gold nanoparticles with spin coating. In order to generate a high-quality layer of nanoparticles, we used the spin-coating approach developed by Jiang et al.[15] Briefly, the process has two different acceleration speeds. At the low acceleration speed 200 rpm/sec, the spin coating stayed at 200 rpm for 120 s, 300 rpm for 120 s, 1000 rpm for 60 s, and 3000 rpm for 20 s. At the high acceleration speed 1000 rpm/sec, the spin coating continued at 6000 rpm for 20 s and finally at 8000 rpm for 360 s. After being soft baked around 60 $^{\circ}C$ for 15 minutes, the wafer slowly cooled down to the room temperature and is ready to serve as the stamp in the subsequent inverse nanotransfer printing.

Structured super-hydrophobic surfaces in PDMS were fabricated by soft lithography techniques.[24,25] The soft lithography technique can be applied to produce patterns on the micrometer- and nanometer-length scales. Here we used a DVD disc to create patterned surfaces in PDMS. The DVD disc has a patterned structure with holes, and serves as the mold. The PDMS solution was poured over the DVD disc under vacuum to remove bubbles and then baked at 60 $^{\circ}C$ for 1 hour. In our practice, the degree of curing was 30% lower than that of a typical soft lithographic curing procedure. In other words, our PDMS surface was not fully cured. We found out that 70% curing can effectively help to reach the conformal adhesion between the PDMS surface and gold nanoparticles for better nanotransfer printing.

With the PDMS structured surface, we can begin the process of the inverse nanotransfer printing (Figure 1b). We placed the PDMS surface on top of the silicon stamp under high

vacuum (9.5×10^{-4} Pa) for three hours, to achieve intimate, conformal contact and adhesion between the raised regions of the PDMS surface and the silicon stamp. Then we baked them for six hours at 60 $^{\circ}C$ to further promote the adhesion of nanoparticles to the raised regions of the PDMS surface. Finally, we peeled the structured PDMS surface and the stamp apart. Nanoparticles were transferred from the stamp to the PDMS surfaces. Figure 2a and 2b show the AFM images of the PDMS structured surfaces with and without nanoparticles.

It was demonstrated that hierarchical surfaces with nanoroughness can effectively suppress the Cassie-Wenzel transition and improve the super-hydrophobicity.[10–13] To examine whether our fabricated hierarchical structure can increase the super-hydrophobicity, we carried out experiments on the evaporation of sessile droplets over structured surfaces with and without nanoparticles. The process of a freely evaporating droplet on a super-hydrophobic surface is intriguing.[26,27] Initially, the droplet over a structured surface is in the Cassie state where air bubbles are trapped inside the rough surface underneath the droplet,[1] leading to a high contact angle. The decrease of the droplet size, due to the natural evaporation, results in a larger Laplace inner pressure, which can drive the droplet into a fully wetting (Wenzel) state.[9]

The evaporation process was conducted at room temperature (21 ± 1 $^{\circ}C$) with a relative humidity $22\pm2\%$. The used water was ultrapurified with a specific resistivity of 18.2 $\mathrm{M\Omega\,cm}$ (PURELAB Classic, ELGA LabWater, LLC). The initial droplet volume was 2 μL. The side-view images of the evaporating droplet were recorded. Figure 3 plots the snapshots of time-dependent evaporating droplets over the hierarchical super-hydrophobic surface. The volume of the droplet and the contact angle were measured against the time by a plug-in for ImageJ that uses low-bond axisymmetric drop shape analysis.[28,29]

Figure 4a plots the macroscopic contact angle θ as a function of time during the process of the natural evaporation for the super-hydrophobic surfaces with nanoparticles (the solid line) and without nanoparticles (the dashed line). Figure 4b shows the normalized droplet volume V/V_0 where V_0 is the initial volume as a function of the normalized time $(t_f - t)/t_f$ in which t_f is the total droplet life time in the natural evaporation. The solid line is the power-law relation ($V(t) \sim (t_f - t)^{3/2}$). This law is the result of a pure diffusive evaporation,[30] which corresponds to the evaporation of the droplet with a constant contact angle where the contact line recedes and the droplet self-similarly reduces its volume. The droplet with the Cassie state maintains its quasi-spherical shape during the evaportation.[5] Once the transition to the Wenzel state occurs, the contact line is pinned and the data deviates from this power-law relation. Evidently, Figure 4b shows that nanoparticles on the super-hydrophobic surface effectively delay the Cassie-Wenzel transition which is also confirmed by the time-dependence contact-angle dynamics in Figure 4a. The contact angle over a hierarchical surface maintains a constant value for a longer period time compared to that over a standard super-hydrophobic surface.

In addition, we also examined the contact angle hysteresis by depositing a droplet over a tilted surface and observing the droplet's motion. Figure 5 shows that the droplet slides on the super-hydrophobic surface with nanoparticles at a low roll-off angle ($\alpha = 3.0^\circ$). Our designed hierarchical super-hydrophobic surface with nanoparticles demonstrates a very low contact angle hysteresis $\Delta\theta < 2.5^\circ$. The low contact angle hysteresis and low sliding angle indicate that the super-hydrophobic surface with nanoparticles has extraordinary water repellency.

Finally, to prove the concept of biosensing, we deposited droplets with different-concentration rhodamine 6G over both the glass substrate and the silica-coated gold nanoparticle-based super-hydrophobic surface. After the droplets completely dried out, we measured the Raman signals using the LabRAM HR Raman microscope (HORIBA Jobin Yvon) with the 514.32 nm excitation laser (Figure 6) and examined the SERS sensitivity of our designed super-hydrophobic surface with nanoparticles. For the glass substrate, the Raman scattering cannot be detected for 10^{-9} M of rhodamine 6G. In contrast, even for 10^{-12} M, we still can capture the Raman intensity peak for the super-hydrophobic surface with nanoparticles, which is the orders of magnitude improvement. In other words, our fabricated surface has the potential for high-sensitive molecule detection.

In summary, a simple fabrication technique combining both spin coating and inverse nanotransfer printing provides an inexpensive means of transferring silica-coated metallic nanoparticles onto super-hydrophobic surfaces made of PMDS over large areas. More specifically, we transferred silica-coated gold nanoparticles to fabricate the hierarchical super-hydrophobic surface. Measuring the contact angle and observing the natural evaporation of a sessile droplet demonstrated that the fabricated nanoparticle-based super-hydrophobic surface effectively improves the super-hydrophobicity. In addition, the SERS measurements suggested that the fabricated nanoparticle-based super-hydrophobic surface can significantly enhance the Raman signals. This approach can find important technological applications in biosensing.

Acknowledgements

This work was, in part, supported by the National Science Foundation under Grant No. ECCS-1509866.

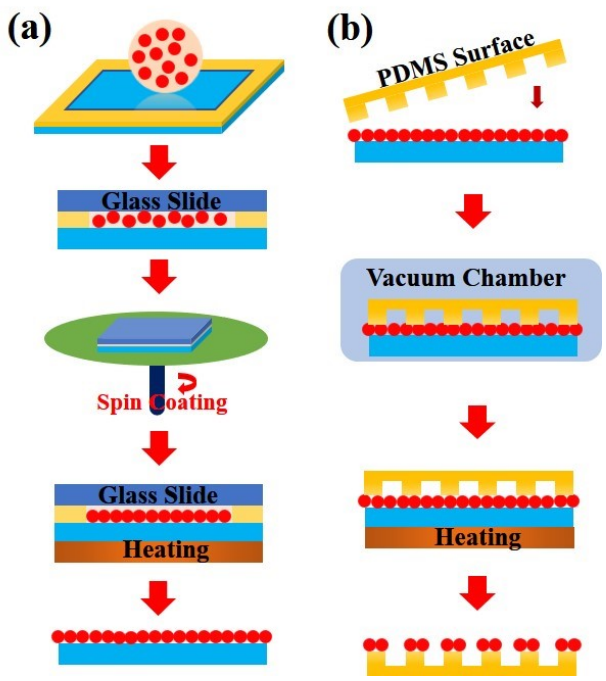

Figure 1. Schematics of procedures of (a) using the spin coating to make a layer of gold nanoparticles; (b) using the inverse nanotransfer printing method to transfer metallic nanoparticles to the raising regions of the PDMS structured surface.

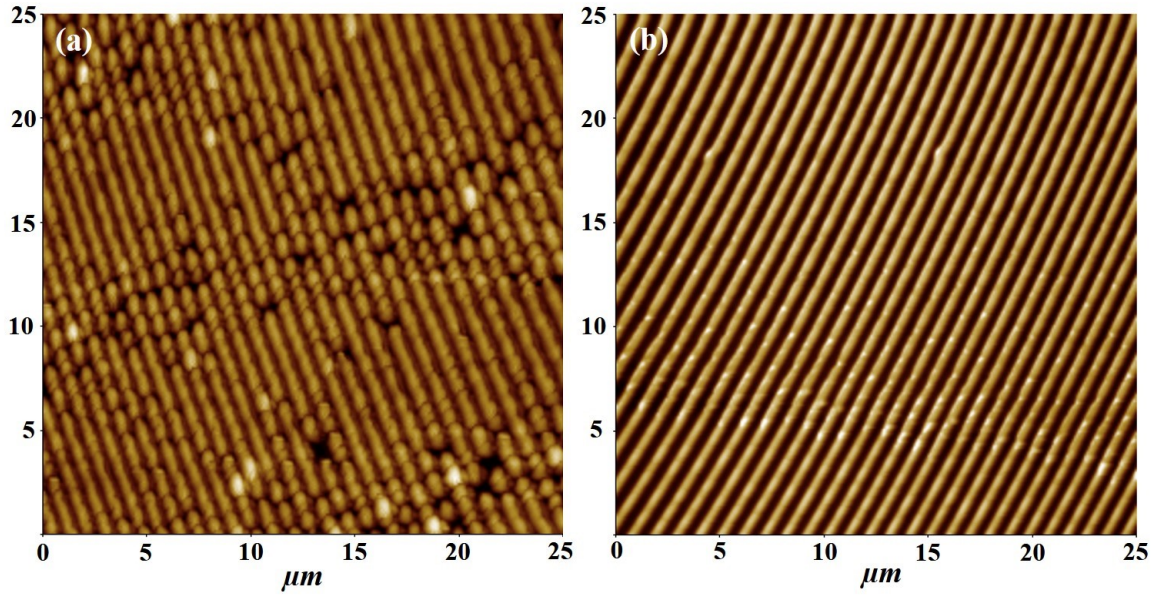

Figure 2. AFM images of the structured PDMS surfaces without nanoparticles (a); and with nanoparticles (b).

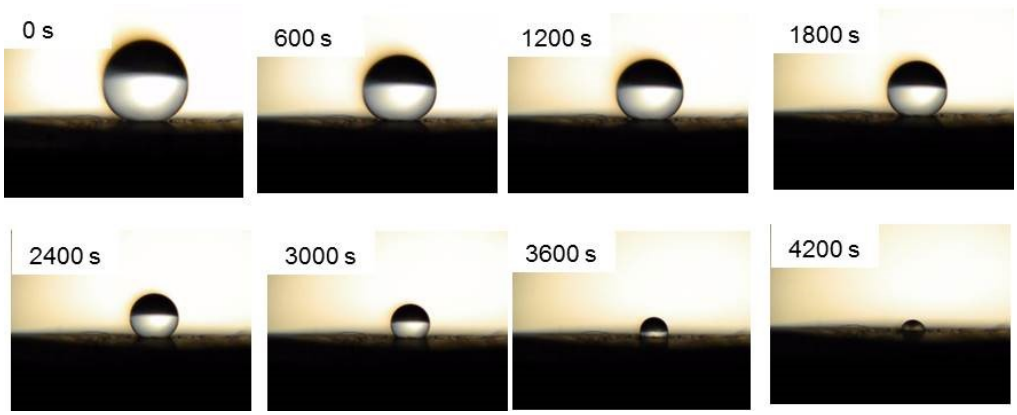

Figure 3. Snapshots of an evaporating droplet with the time interval 600 s.

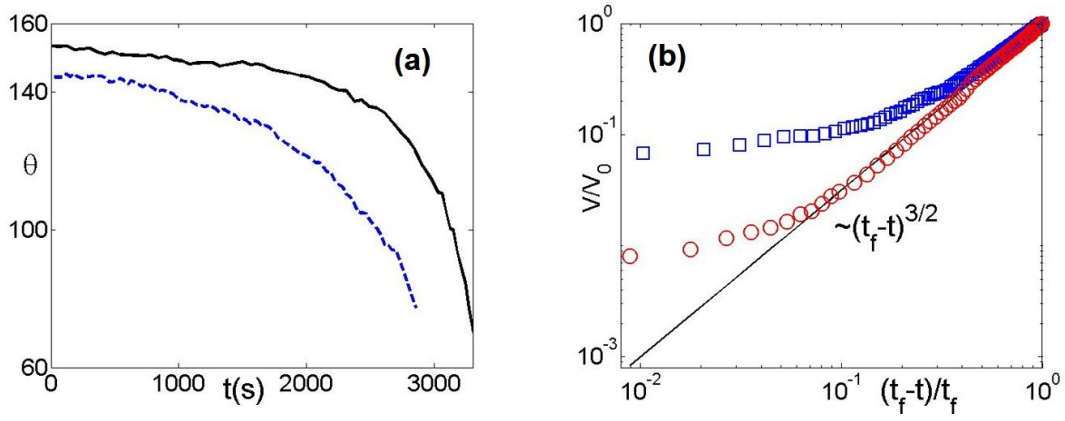

Figure 4. (a) Time evolutions of the contact angles θ of an evaporating sessile water droplet on super-hydrophobic surfaces with nanoparticles (the solid line) and without nanoparticles (the dashed line); (b) The corresponding normalized droplet volumes V/V_0 as a function of the normalized time $(t_f - t)/t_f$ for the one with nanoparticles (circles) and that without nanoparticles (squares).

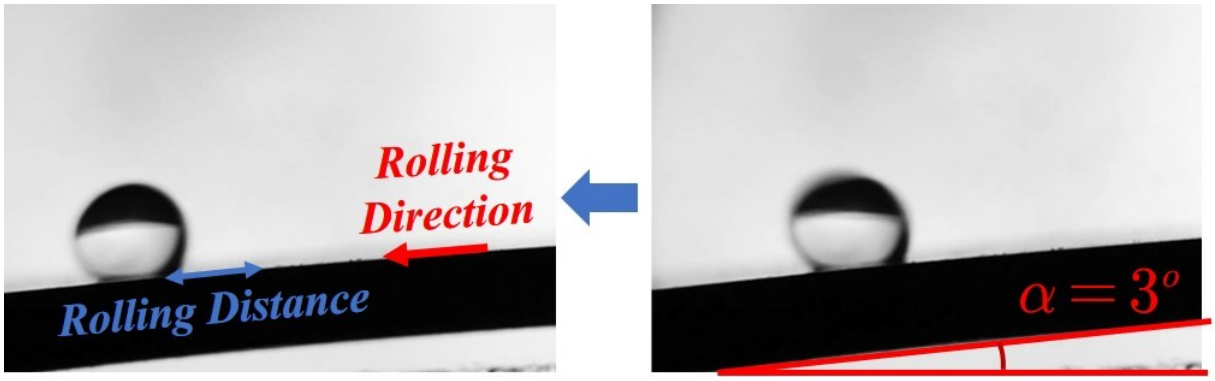

Figure 5. Optical images demonstrating the water droplet (2 µl) mobility sliding on the super-hydrophobic surface with nanoparticles at a low roll-off angle ($\alpha = 3.0^\circ$).

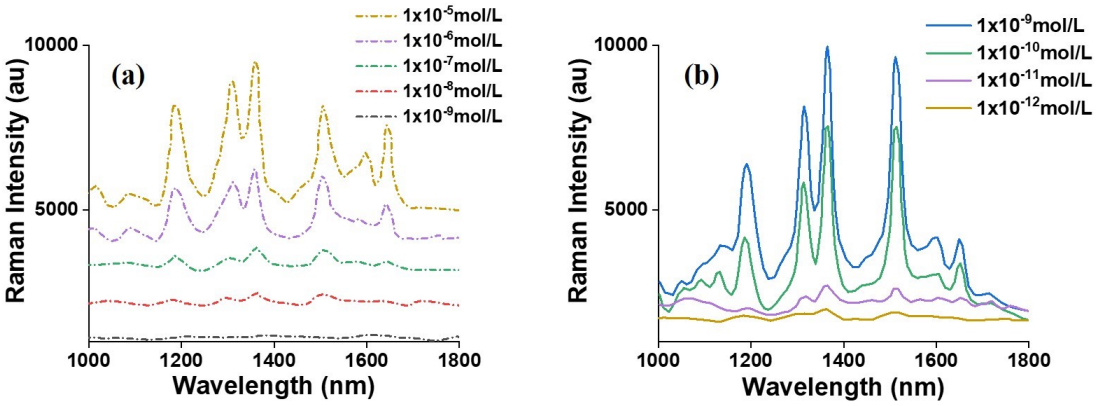

Figure 6. Raman spectra of rhodamine 6G with various concentrations deposited on the glass substrate (a) and the super-hydrophobic surface with nanoparticles (b).

References:

[1] J.P. Rothstein, Annual Review of Fluid Mechanics **42**, 89 (2010).

[2] L. Bocquet and E. Lauga, Nature Materials **10**, 334 (2011).

[3] C. Cottin-Bizonne, J.-L. Barrat, L. Bocquet, and E. Charlaix, Nature Materials **2**, 237 (2003).

[4] N.A. Patankar, Soft Matter **6**, 1613 (2010).

[5] F. De Angelis, F. Gentile, F. Mecarini, G. Das, M. Moretti, P. Candeloro, M.L. Coluccio, G. Cojoc, A. Accardo, C. Liberale, R.P. Zaccaria, G. Perozziello, L. Tirinato, A. Toma, G. Cuda, R. Cingolani, and E. Di Fabrizio, Nature Photonics **5**, 682 (2011).

[6] P. Kim, M.J. Kreder, J. Alvarenga, and J. Aizenberg, Nano Letters **13**, 1793 (2013).

[7] F. Gentile, M. Moretti, T. Limongi, A. Falqui, G. Bertoni, A. Scarpellini, S. Santoriello, L. Maragliano, R. Proietti Zaccaria, and E. di Fabrizio, Nano Letters **12**, 6453 (2012).

[8] J. Zhu, Ş.K. Özdemir, and L. Yang, Nature Photonics **5**, 653 (2011).

[9] A. Lafuma and D. Quéré, Nature Materials **2**, 457 (2003).

[10] L. Gao and T.J. McCarthy, Langmuir : the ACS Journal of Surfaces and Colloids **22**, 6234 (2006).

[11] J. Feng, M.T. Tuominen, and J.P. Rothstein, Advanced Functional Materials **21**, 3715 (2011).

[12] R. Raj, R. Enright, Y. Zhu, S. Adera, and E.N. Wang, Langmuir : the ACS Journal of Surfaces and Colloids **28**, 15777 (2012).

[13] S. Zhai, Y. Zhao, and H. Zhao, ACS Appl. Mater. Interfaces **11**, 12978 (2019).

[14] P. Jiang and M.J. McFarland, Journal of the American Chemical Society **126**, 13778 (2004).

[15] P. Jiang, T. Prasad, M.J. McFarland, and V.L. Colvin, Applied Physics Letters **89**, 011908 (2006).

[16] N.C. Linn, C.-H. Sun, P. Jiang, and B. Jiang, Applied Physics Letters **91**, 101108 (2007).

[17] P. Jiang, C.-H. Sun, N.C. Linn, B.J. Ho, and S. Venkatesh, Current Nanoscience **3**, 296 (2007).

[18] Y.-L. Loo, R.L. Willett, K.W. Baldwin, and J.A. Rogers, Applied Physics Letters **81**, 562 (2002).

[19] M.A. Meitl, Z.-T. Zhu, V. Kumar, K.J. Lee, X. Feng, Y.Y. Huang, I. Adesida, R.G. Nuzzo, and J.A. Rogers, Nature Materials **5**, 33 (2005).

[20] T.-H. Kim, A. Carlson, J.-H. Ahn, S.M. Won, S. Wang, Y. Huang, and J.A. Rogers, Applied Physics Letters **94**, 113502 (2009).

[21] A. Carlson, A.M. Bowen, Y. Huang, R.G. Nuzzo, and J.A. Rogers, Advanced Materials (Deerfield Beach, Fla.) **24**, 5284 (2012).

[22] J.A. Rogers, Science **337**, 1459 (2012).

[23] J.C. Hulteen, Journal of Vacuum Science & Technology A: Vacuum, Surfaces, and Films **13**, 1553 (1995).

[24] Y. Xia and G.M. Whitesides, Annual Review of Materials Science **28**, 153 (1998).

[25] J.C. McDonald, D.C. Duffy, J.R. Anderson, D.T. Chiu, H. Wu, O.J. Schueller, and G.M. Whitesides, Electrophoresis **21**, 27 (2000).

[26] P. Tsai, R.G.H. Lammertink, M. Wessling, and D. Lohse, Physical Review Letters **104**, 116102 (2010).

[27] X. Chen, R. Ma, J. Li, C. Hao, W. Guo, B.L. Luk, S.C. Li, S. Yao, and Z. Wang, Physical Review Letters **109**, 129904 (2012).

[28] A.F. Stalder, G. Kulik, D. Sage, L. Barbieri, and P. Hoffmann, Colloids and Surfaces A: Physicochemical and Engineering Aspects **286**, 92 (2006).

[29] A.F. Stalder, T. Melchior, M. Müller, D. Sage, T. Blu, and M. Unser, Colloids and Surfaces A: Physicochemical and Engineering Aspects **364**, 72 (2010).

[30] A.-M. Cazabat and G. Guéna, Soft Matter **6**, 2591 (2010).